ACES Asian Chemical Editorial Society

DOI: 10.1002/asia.202100037

CHEMISTRY
AN ASIAN JOURNAL
Full Paper

Special Collection

Controlling Energy Gaps of π-Conjugated Polymers by Multi-Fluorinated Boron-Fused Azobenzene Acceptors for Highly Efficient Near-Infrared Emission

Masayuki Gon, Junko Wakabayashi, Masashi Nakamura, Kazuo Tanaka,* and Yoshiki Chujo[a]

Abstract: We demonstrate that multi-fluorinated boron-fused azobenzene (BAz) complexes can work as a strong electron acceptor in electron donor-acceptor (D-A) type π-conjugated polymers. Position-dependent substitution effects were revealed, and the energy level of the lowest unoccupied molecular orbital (LUMO) was critically decreased by fluorination. As a result, the obtained polymers showed near-infrared (NIR) emission ($\lambda_{PL} = 758$–847 nm) with high absolute photoluminescence quantum yield ($\Phi_{PL} = 7$–23%) originating from low-lying LUMO energy levels of the BAz moieties (−3.94 to −4.25 eV). Owing to inherent solid-state emissive properties of the BAz units, deeper NIR emission ($\lambda_{PL} = 852980$ nm) was detected in film state. Clear solvent effects prove that the NIR emission is from a charge transfer state originating from a strong D-A interaction. The effects of fluorination on the frontier orbitals are well understandable and predictable by theoretical calculation with density functional theory. This study demonstrates the effectiveness of fluorination to the BAz units for producing a strong electron-accepting unit through fine-tuning of energy gaps, which can be the promising strategy for designing NIR absorptive and emissive materials.

1. Introduction

Growing demands for high performance and sophisticated materials require finely predictable and controllable design strategies for constructing functional organic compounds. As one of the candidates for designable organic materials, π-conjugated polymers have attracted much attention owing to unique characteristics, such as intense luminescence, high electrical conductivities and good film-formability.[1] The energy gaps, which are defined as a width of the energy levels between a highest occupied molecular orbital (HOMO) and a lowest unoccupied molecular orbital (LUMO), are critical factors for determining the material properties.[2] In particular, electron donor-acceptor (D-A) type π-conjugated polymers composed of an alternating array of electron-donor and acceptor moieties have actively studied by feature of easily controllable energy gaps with selecting a donor and an acceptor having desired HOMO and LUMO energy levels as co-monomers, respectively. From these utilities, D-A type π-conjugated polymers have been often applied to organic light-emitting diodes (OLEDs),[3] organic field effect transistors (OFETs)[4] and organic photovoltaics (OPVs).[5] Hence, the development of novel compounds showing electron-donating and accepting abilities is still necessary for preparing D-A type π-conjugated polymers.

Narrow energy gaps of the D-A type π-conjugated polymers can be an origin of absorption and emission in the near-infrared (NIR) region and those were significant for effective use of sun light for organic film solar cells[6] and bioimaging, optical communication.[7] In order to construct stable π-conjugated polymers having the narrow energy gaps, reduction of a LUMO energy level of an acceptor unit is required because elevation of a HOMO energy level has a risk of oxidation by air under ambient conditions.[8] One of the strategies for lowering the LUMO energy level is the introduction of fluorine substituents to the acceptor.[9] A fluorine atom intrinsically has high electron negativity and is inactive to chemical substances. Fluorination enhances electron-accepting ability of the organic compounds with good chemical stability.

Recently, we proposed the concept of "element-blocks", which are structural functional units consisting of various groups of elements, to create advanced materials.[10] According to the concept, we revealed that boron-fused azobenzene/azomethine (BAz/BAm) complexes, which are "element-blocks" constructed mainly by B, N, O, C and H, worked as a strong acceptor in D-A type π-conjugated polymers with highly efficient emissions including NIR region both in solution and film states.[11] The film-state emission is valuable because the emission is generally spoiled in a condensed state due to loss of excitation energy via non-radiative pathway mainly by intermolecular π–π interaction.[12] One of the reasons of the film-state emission could be attributable to the fact that the BAz/BAm complexes potentially enhanced their emission in solid or crystalline states although the emission is critically quenched in the diluted solution state.[13] These phenomena are known as aggregation-induced emission (AIE)[14] or crystallization-induced emission enhancement (CIEE) properties.[15]

Herein, to reinforce electron-accepting ability of the BAz skeleton, we synthesized fluorinated BAz complexes and

---

[a] *Dr. M. Gon, J. Wakabayashi, M. Nakamura, Prof. Dr. K. Tanaka, Prof. Dr. Y. Chujo*
Department of Polymer Chemistry, Graduate School of Engineering
Kyoto University Katsura, Nishikyo-ku, Kyoto 615-8510 (Japan)
E-mail: tanaka@poly.synchem.kyoto-u.ac.jp

Supporting information for this article is available on the WWW under https://doi.org/10.1002/asia.202100037

This manuscript is part of a special collection dedicated to Early Career Researchers.

corresponding D-A type π-conjugated polymers with bithiophene units as a donor. Azobenzene scaffolds were chosen by their inherent higher electron-accepting abilities than azomethine ones to prepare strong acceptors aiming to deeper NIR absorption and emission.[16] As a result, the LUMO energy levels, which are one of the indexes evaluating the degree of acceptors, were lowered depending on the number of introduced fluorine atoms with the BAz complexes. The obtained D-A type π-conjugated polymers showed highly-efficient NIR emission ($\lambda_{PL}=758\sim847$ nm) in diluted solution and moderate NIR emission ($\lambda_{PL}=852\sim980$ nm) in film state. The solvent effects evaluated by Lippert-Mataga plots proved that the polymers formed clear D-A interactions. Moreover, the experimental data were good agreement with the results of theoretical calculations by density functional theory (DFT), and therefore the properties were predictable. We proposed that the high designability of D-A type π-conjugated polymers by fluorination with BAz complexes was good example for constructing desired functional materials having controllable energy gaps.

2.1 Synthesis

Scheme 1 shows the syntheses of three types of fluorinated BAz complexes modified with the fluorine atoms at 3,3′ positions (**BAz-3F**), 5,5′ positions (**BAz-5F**) and both 3,3′ and 5,5′ positions (**BAz-35F**). The pristine BAz complex, **BAz**, was prepared according to our previous report.[11b] The fluorinated BAz complexes, **BAz-3F**, **BAz-5F**, and **BAz-35F**, were isolated in high yields by the condensation reaction at 100 °C in toluene between the corresponding azobenzene tridentate ligands, **Az-3F-OH**, **Az-5F-OH** and **Az-35F-OH**, and boron trifluoride diethyl etherate ($BF_3{\cdot}Et_2O$), respectively. Next, by using the obtained BAz complexes as monomers, D-A type π-conjugated copolymers with a bithiophene co-monomer were synthesized (Scheme 2 and Table 1). Migita-Kosugi-Stille cross-coupling polymerizations[17] with **BAz-3F**, **BAz-5F** or **BAz-35F** and 5,5′-bis(trimethylstannyl)-3,3′-didodecyl-2,2′-bithiophene (**BT**) were executed in a catalytic system involving $Pd_2(dba)_3$ (dba = dibenzylideneacetone) and 2-dicyclohexylphosphino-2′,4′,6′-triisopropylbiphenyl (XPhos) to afford target copolymers, **P-BAz-3F**, **P-BAz-5F** or **P-BAz-35F**, respectively. The synthetic results and polymer data are listed in Table 1. In the case of **P-BAz-5F** and **P-BAz-35F**, high molecular weight polymers were fractionated by high performance liquid chromatography (HPLC) in chloroform as an eluent. In this research, the synthetic polymer data of **P-BAz** were cited or recollected as comparison.[11b,d,e] All synthesized compounds showed good solubility in common organic solvents such as toluene, chloroform, dichloromethane and tetrahydrofuran, and can be characterized by ^{1}H, ^{13}C, ^{11}B NMR, MS spectra (see Supporting Information). From those characterization data, we concluded that the samples have the objective structures and enough purity for further analyses.

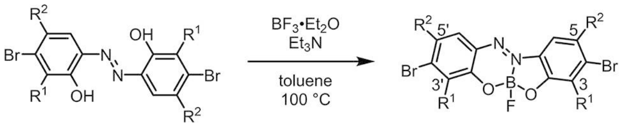

Az-OH (R^1 = H, R^2 = H)
Az-3F-OH (R^1 = F, R^2 = H)
Az-5F-OH (R^1 = H, R^2 = F)
Az-35F-OH (R^1 = F, R^2 = F)

BAz (R^1 = H, R^2 = H), 77%
BAz-3F (R^1 = F, R^2 = H), 86%
BAz-5F (R^1 = H, R^2 = F), 77%
BAz-35F (R^1 = F, R^2 = F), 96%

Scheme 1. Syntheses of monomers, **BAz**, **BAz-3F**, **BAz-5F** and **BAz-35F** with the name of substitution positions.

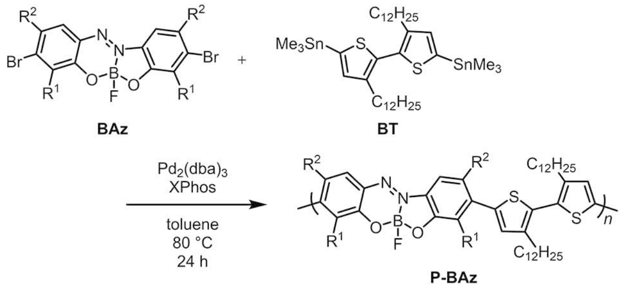

Scheme 2. General procedure for polymer synthesis.

2.2 Optical measurements

To investigate the position-dependent substituent effect of fluorine atoms on the electronic situation in the ground state, UV-vis absorption measurements were executed in the diluted chloroform solutions (1.0×10^{-5} M) (Figures 1 and S1, Table 2).

Table 1. Molecular weights and isolated yields of the synthesized polymers.

	R^1	R^2	M_n[a] /kDa	M_w[a] /kDa	M_w/M_n	yield /%
P-BAz-F [b]	H	H	21.4	55.6	2.5	85
P-BAz-3F	F	H	13.8	38.8	3.2	54
P-BAz-5F [c]	H	F	24.5	48.5	2.0	54
P-BAz-35F [c]	F	F	13.4	20.8	1.6	44

[a] Determined by a gel permeation chromatography (GPC) with polystyrene standards. [b] ref 11b. [c] After fractionated by HPLC.

Table 2. Optical data of the BAz monomers and polymers in solution and solid or film states.

	solution			solid or film		
	λ_{abs}[a]/ nm	λ_{PL}[b]/ nm	Φ_{PL}[b,c] /%	λ_{abs}[d]/ nm	λ_{PL}[d]/ nm	Φ_{PL}[c,d]/ %
BAz	486	621	<1	–	645	7
BAz-3F	480	644	<1	–	613	2
BAz-5F	513	654	<1	–	637	6
BAz-35F	510	688	<1	–	644	2
P-BAz	631	758	23	660	852	4
P-BAz-3F	643	794	8	682	926	<1
P-BAz-5F	666	821	11	698	916	<1
P-BAz-35F	670	847	7	717	980	<1

[a] 1.0×10^{-5} M for monomers and 1.0×10^{-5} M per repeating unit for polymers in $CHCl_3$. [b] 1.0×10^{-5} M for monomers and 1.0×10^{-5} M per repeating unit for polymers in toluene, excited at absorption maxima for PL. [c] Absolute PL quantum yield excited at absorption maxima. [d] Solid state for monomers and spin-coated film on the quartz substrate (0.9 cm × 5 cm) prepared from chloroform solution (0.10 mL, 1000 rpm, concentration: 1.0 mg/0.30 mL) for polymers; excited at absorption maxima for PL.

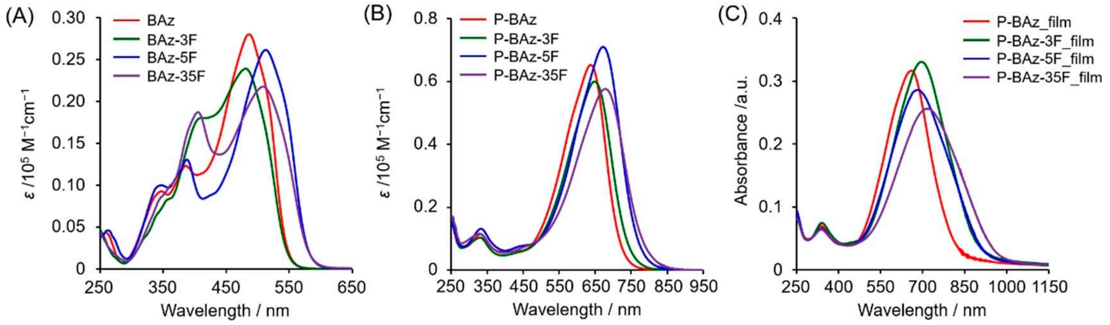

Figure 1. UV-vis absorption spectra of (A) BAz monomers, (B) polymers in chloroform (1.0×10^{-5} M for monomers, 1.0×10^{-5} M per repeating unit for polymers) and (C) polymer films.

Interestingly, it was found that the substituent effects worked independently. By substitution at 3,3′ positions, the middle transition bands at around 400 nm raised and the energy gaps were preserved (Figures 1A and S1 A). On the other hand, the bathochromic shifts of absorption spectra were observed by substitution at 5,5′ positions with retaining almost the same spectra shape. Furthermore, the two different effects had additive property and **BAz-35F** showed both substitution effects at 3,3′ and 5,5′ positions. As a result, **BAz** and **BAz-3F** or **BAz-5F** and **BAz-35F** had the same energy gap, respectively, and the bathochromic shifts of absorption spectra were detected in **BAz-5F** and **BAz-35F** compered to **BAz** and **BAz-3F** (Figures 1A and S1 A).

In the D-A type π-conjugated polymers, the absorption bands were located at the longer wavelength regions than those of the corresponding monomers (Figures 1A and 1B). Contrary to the monomers, the value of absorption maximum wavelength (λ_{abs}) was larger in the order of **P-BAz-35F**, **P-BAz-5F**, **P-BAz-3F** and **P-BAz**. Considering that electron-accepting ability of a compound is enhanced by fluorination, the order should be correlated to the strongness of D-A interaction between BAz and bithiophene units. In other words, the ability of BAz acceptors was able to be reinforced by fluorination. Moreover, homogeneous thin films were easily prepared by the commodity spin-coated method because of good film-formability of the synthesized polymers. The slight bathochromic shifts and broader absorption bands were observed in the film samples compared to those in the diluted solutions (Figures 1B and 1 C, Table 1). Owing to the strong D-A interaction leading to a narrow energy gap, the absorption maximum reached a NIR region.

To investigate electronic situations of the BAz complexes in the excited state, the photoluminescence (PL) properties were evaluated in toluene (1.0×10^{-5} M) and in crystal (Figure 2 and Table 1). It was clearly demonstrated that AIE or CIEE properties were obtained from the complexes. The emission intensity was obviously very weak in solution ($\Phi_{PL}<1\%$), whereas intense emission was monitored in crystal ($\Phi_{PL}=2\sim7\%$) (Figure 2A and 2B). Our previous work proposed that the emission quenching in diluted solution should be caused by excitation-driven bending motions which promote non-radiative excitation decay.[11a,b,13a,18] In solid or crystal packing, those molecular motions are effectively restricted and therefore the emission should be recovered. These situations were often shown in the series of tetracoordinated boron with the azobenzene/azomethine-based tridentate ligands and those compounds also exhibited AIE or CIEE properties.[11,13]

Contrary to the monomers with environment-sensitive luminescent properties, intense NIR emission was observed from the polymers even in the diluted solution (Figures 2C, 2D and Table 1). The order of the maximum PL wavelength (λ_{PL}) was the same with that of the λ_{abs}. The λ_{PL} and Φ_{PL} were 758~847 nm and 7~23%, respectively, and it was shown that the BAz scaffold should be good candidate for NIR-emissive “element-blocks”. Since the excitation-driven molecular motions of the monomeric units would be inhibited by incorporating into the polymer chains,[11a,b,18] the intense emission should be induced in diluted solution. In the films, the BAz polymers also showed emission in the NIR region (Figure 2D and Table 1). **P-BAz** showed intense emission even in the film ($\lambda_{PL}=858$ nm, $\Phi_{PL}=4\%$).[11b,e] Although the other polymers exhibited weak emission ($\Phi_{PL}<1\%$), however the λ_{PL}s were detectable at 916~980 nm. Therefore, it can be said that BAz unit has potential to targeting to fabricate functional materials showing deeper NIR emission.

2.3 Solvent effects

To obtain more insight about the D-A system originating from strong electron-accepting ability of fluorinated BAz units, we investigated solvent effects on UV-vis-NIR absorption and PL spectra. All the spectroscopic data are shown in Figures S2 and S3, Tables S1 and S2. From the Lippert-Mataga plot of BAz monomers in three types of solvents, toluene ($\Delta f=0.013$, Δf: orientation polarizability), chloroform ($\Delta f=0.15$) and dichloromethane ($\Delta f=0.22$), there were almost no correlations between Δf and Stokes shift (v) ($R^2<0.50$, R: correlation coefficient) (Figure 3A). This means that the emission of BAz monomer is not from a charge transfer (CT) state but from a localized electronic (LE) state. On the other hand, BAz polymers had good correlations ($R^2>0.90$) between Δf and v by using five types of the solvent including benzene ($\Delta f=0.003$) and chlorobenzene ($\Delta f=0.14$) (Figure 3B). Although we also eval-

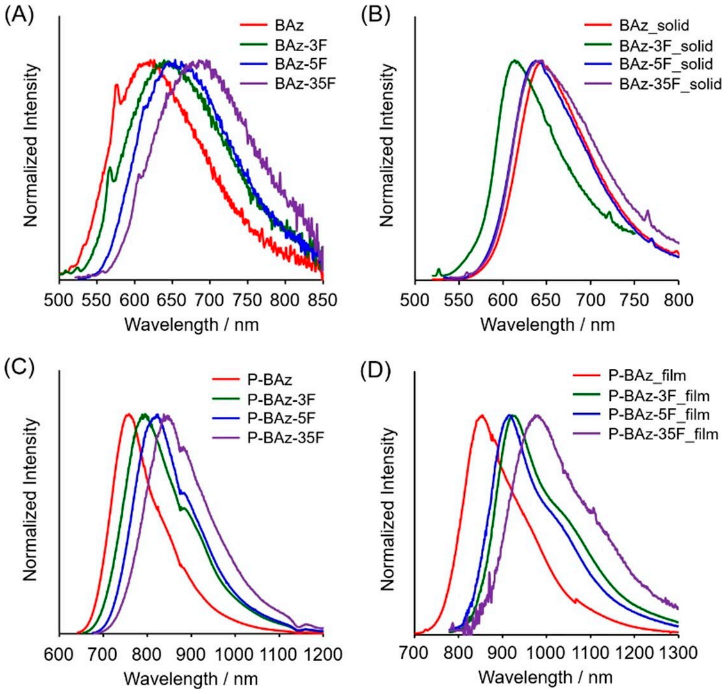

Figure 2. PL spectra of BAz monomers (A) in chloroform (1.0×10^{-5} M) and (B) in solid state, BAz polymers (C) in chloroform (1.0×10^{-5} M per repeating unit) and (D) in film state with the excitation light at each absorption maximum.

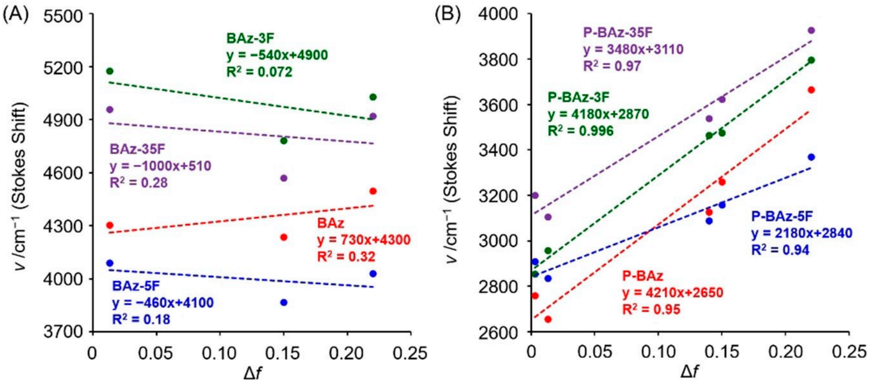

Figure 3. Lippert-Mataga plots of (A) BAz monomers and (B) polymers in the diluted solutions (1.0×10^{-5} M for monomers and 1.0×10^{-5} M per repeating unit for polymers) at room temperature. The formulas of approximate straight lines are described in the same figures. Plotted data are listed in Tables S1 and S2.

uated the solvent effect in tetrahydrofuran ($\Delta f = 0.21$), the emission band was observed in a position separated from expectation (Figure S4). This might be because nucleophilicity of THF originating from lone pairs of oxygen affected the boron atom in addition to the solvent effect. The slopes of the approximation straight lines in Lippert-Mataga plots were almost the same, while those tended to be decreased by fluorination at 5,5′ positions.

During the investigation of the solvent effects, we found generation of the unique absorption band from 700 to 900 nm only from **P-BAz-3F** in benzene/chloroform, toluene/chloroform or dichloromethane/chloroform = 99/1 v/v mixed solutions (Figure S3). From the variable temperature (VT) UV-vis-NIR absorption measurements in toluene/chloroform = 99/1 v/v solution, the band gradually decreased by increasing temperature and subsequently disappeared at 50 °C (Figure S5A). Subsequently, the band was recovered by a cooling process and finally the original spectrum was reproduced at 10 °C (Figure S5B). Interestingly, the hysteresis was observed by holding each temperature for 10 minutes per 10 °C (Figure S5C). The disappearance and reproduction of the band slowly proceeded by monitoring at 40 °C under heating and cooling processes, respectively (Figure S5D). High reversibility was obtained at least five times (Figure S5E) and the hysteresis behavior was reproducible. Furthermore, weak NIR emission at around 950 nm was detectable by excitation at the absorption band (Figure S5F). In the case of the other polymers, **P-BAz**, **P-BAz-5F** and **P-BAz-35F**, there was no unusual temperature dependency regardless of the presence or absence of fluorine substituents (Figure S6).[19] The generation of the band in longer wavelength

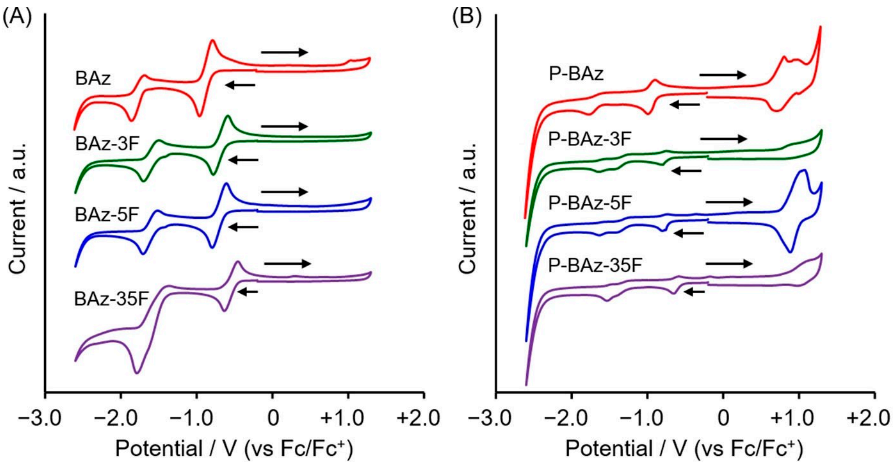

Figure 4. Cyclic voltammograms of (A) BAz monomers and (B) BAz polymers in dichloromethane (1.0×10^{-3} M for monomers, 1.0×10^{-3} M per repeating unit for polymers) containing $n\mathrm{Bu_4NPF_6}$ (0.10 M) at room temperature with a scan rate of 0.1 V $\mathrm{s^{-1}}$ (negative scan). The black arrows denote sweep directions (negative scan).

region could be derived from intra- or intermolecular π–π interaction of the polymer chains of **P-BAz-3F** in solution although significant aggregation was not suggested from a dynamic light scattering (DLS) data.[20] According to the crystal packing structures of **BAz** and **BAz-3F**, it was suggested that the fluorine atom at 3′ position is responsible for intermolecular interaction between two molecular fractions of **BAz-3F** (Figures S7~S9, Tables S3 and S4). In particular, there were three short contacts in **BAz-3F** and they were shorter than those of **BAz**, respectively (Figure S9). As a result of the strong binding, the molecules of **BAz-3F** were able to have almost planar conformation in the condensed state. Relatively-planar conformation might be favorable for the formation of assembly followed by the generation of the new absorption band in solution.

Table 3. Energy levels of molecular orbitals of BAz monomers and polymers.

	$\lambda_{\mathrm{abs,edge}}{}^{a}$/ nm	$E_{\mathrm{g,opt}}{}^{b}$/ eV	$E_{\mathrm{onset}}{}^{\mathrm{red}\ c}$/ V	$E_{\mathrm{LUMO}}{}^{d}$/ eV	$E_{\mathrm{HOMO}}{}^{d}$/ eV
BAz	546	2.27	−0.80	−4.00	−6.27
BAz-3F	546	2.27	−0.61	−4.19	−6.46
BAz-5F	579	2.14	−0.63	−4.17	−6.31
BAz-35F	579	2.14	−0.46	−4.34	−6.48
P-BAz	722	1.72	−0.86	−3.94	−5.66
P-BAz-3F	743	1.67	−0.71	−4.09	−5.76
P-BAz-5F	769	1.61	−0.72	−4.08	−5.69
P-BAz-35F	787	1.58	−0.55	−4.25	−5.83

[a] In chloroform (1.0×10^{-5} M for monomers, 1.0×10^{-5} M per repeating unit for polymers), estimated from Figure S1. [b] $E_{\mathrm{g,opt}}=1240/\lambda_{\mathrm{abs,edge}}$. [c] In dichloromethane (1.0×10^{-3} M for monomers, 1.0×10^{-3} M per repeating unit for polymers) containing $n\mathrm{Bu_4NPF_6}$ (0.10 M) at room temperature with a scan rate of 0.1 V $\mathrm{s^{-1}}$ (negative scan). [d] $E_{\mathrm{LUMO}}=-(4.8-E_{\mathrm{onset}}{}^{\mathrm{red}})$ (eV),[21] $E_{\mathrm{HOMO}}=E_{\mathrm{LUMO}}-E_{\mathrm{g,opt}}$.

2.3 Cyclic voltammetry

To obtain further information on the substituent effect of fluorine atoms on electronic properties, we estimated molecular orbital (MO) energy levels with a cyclic voltammetry (CV). The results are shown in Figure 4 and Table 3. The LUMO energy levels were calculated from the onset of the reduction curve.[21] In both of BAz monomers and polymers, it was found that LUMO energy levels were critically lowered depending on the number of fluorine atoms. In BAz monomers, the HOMO energy levels were not able to be estimated from the cyclic voltammograms because the oxidation peaks were out of the potential window. Therefore, we calculated the HOMO energy levels using optical energy gaps ($E_{\mathrm{g,opt}}$) obtained from the edge of the UV-vis-NIR absorption spectra (Figure S1). It was shown that fluorination at 3,3′ positions, both HOMO and LUMO energy levels were lowered, whereas at 5,5′ positions, only LUMO energy levels were reduced. The similar effect was also monitored in the polymers. The effects had additivity property as shown in the absorption spectra. Accordingly, the electron-accepting ability of BAz unit in the polymer was enhanced up to −4.25 eV in the LUMO energy level of **P-BAz-35F**. Here, although the oxidation peaks were detectable in the voltammograms of BAz polymers, the same estimation method as the monomers was adopted because the values should be compared with the same criteria and the substituent effect should be prominently reflected on the LUMO-localized acceptor moiety. The HOMO energy levels evaluated from the oxidation peaks in the voltammograms are shown in Figure S10 and Table S5. In summary, it was confirmed that energy levels of frontier orbitals can be tuned by fluorination at adequate positions.

2.4 Theoretical calculation

To support experimental results, we carried out theoretical calculation with density functional theory (DFT) and time dependent DFT (TD-DFT) at B3LYP/6-311G(d,p) level. The results are summarized in Figures 5, 6, S11, S12 and Tables S6, S7. In

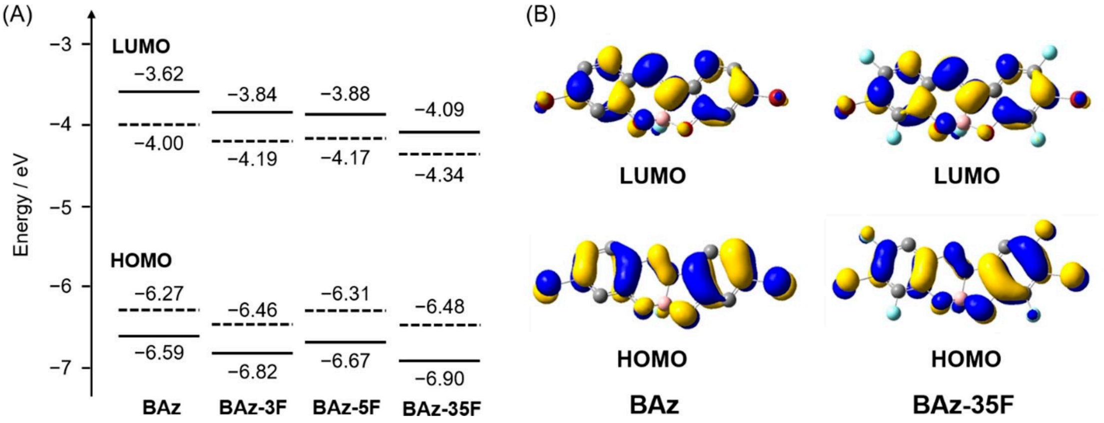

Figure 5. (A) Energy diagrams of BAz monomers (solid line: from DFT calculation, dotted line: from CV and UV-vis absorption spectra, Table 3), (B) HOMO and LUMO of **BAz** and **BAz-35F** obtained from DFT calculations (isovalue = 0.03). Hydrogens were omitted for clarity.

monomers, variation tendency of calculated HOMO and LUMO energy levels was precisely matched to the experimental results (Figure 5A). In LUMO, there were little orbital interaction of fluorine atoms both at 3,3′ and 5,5′ positions, and the only inductive effect of them influenced on energy levels (Figures 5B and S11). Thereby, the step-by-step reduction of LUMO energy levels can be accomplished as increasing the number of fluorine atoms. On the other hand, in HOMO, the orbital interaction of fluorine atoms existed only at 5,5′ positions and electronic donation from the lone pair of fluorine atoms occurred in addition to inductive effect of them (Figure 5B). Hence, elevation of HOMO energy levels was detected in **BAz-5F** and **BAz-35F** (Figure 5A). Consequently, the bathochromic shifts of absorption spectra should be caused by the elevation of HOMO energy levels (Figure 1A and Table S5). We previously reported the similar effect by using bromine atoms as a unique substitution effect at 5,5′ positions of BAz derivatives.[11d] It was noted the orbital interaction at 3,3′ positions was observable in HOMO-2, which led to enhancement of $S_0 \rightarrow S_3$ transition (Figure S11 and Table S6). As a result, rise of the middle absorption band at around 400 nm (Figure 1A) was attributed to the increase of $S_0 \rightarrow S_3$ transition without any disturbance in HOMO-LUMO energy gaps.

To estimate influence of the substituent effect on the electronic structures in polymers, the model compounds having BT units in both sides of the BAz unit were used for calculations (Figures 6, S12 and Table S7). The calculation with model compounds well helped interpreting the situation of the polymers. Contrary to the monomers, BT units worked as donors and the standard HOMO energy levels were dramatically raised (Figure 6A). In polymers, the orbital interaction of fluorine atoms was still effective as shown in the monomers (Figure 6B and S12) and slight elevation of the HOMO energy levels was detected by fluorination at 5,5′ positions (Figure 6A). However, the effect was weakened probably because of large delocalization of HOMO through the BT units (Figure 6B and S12). Meanwhile, relatively localized LUMO was strongly affected by reduction of energy levels through the inductive effect of fluorine atoms. From those effects, the energy gaps were narrower in the order of **P-BAz-35F**, **P-BAz-5F**, **P-BAz-3F**, **P-BAz** (Figure 6A and Table S7). It can be said that the optical properties of the BAz polymers can be finely tuned by selecting the substituent positions.

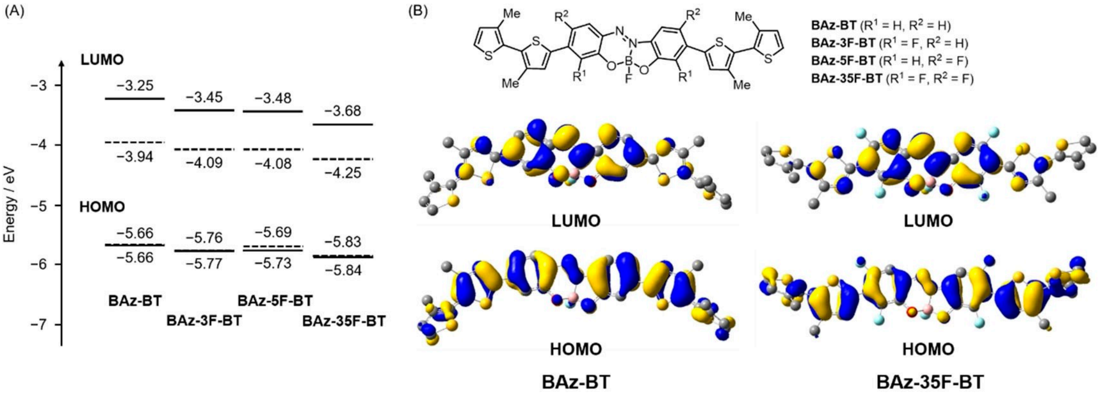

Figure 6. (A) Energy diagrams of model compounds of BAz polymers (solid line: from DFT calculation of model compounds, dotted line: from CV and UV-vis-NIR absorption spectra of BAz polymers, Table 3) and (B) chemical structures of model compounds, and HOMO and LUMO of **BAz-BT** and **BAz-BT-35F** with DFT calculations (isovalue = 0.025). Hydrogens were omitted for clarity.

3. Conclusion

Electronic properties of multi-fluorinated BAz complexes were evaluated. Distinct and different substitution effects at 3,3′ and 5,5′ positions were revealed. Reduction of LUMO energy level was caused by fluorination both at 3,3′ and 5,5′ positions, whereas elevation of HOMO energy level was brought about only by fluorination at 5,5′ positions. The prepared BAz complexes hold potential to solid-state emission with CIEE properties. Owing to strong D-A interaction of π-conjugated polymers with fluorinated BAz and BT units, we obtained highly efficient NIR emission. The energy gaps of the π-conjugated polymers were finely tuned depending on fluorinated positions and numbers; as a result, the maximum emission wavelength reached 847 nm in the diluted solution and 980 nm in the film. Additionally, the solvent effect originating from electronic transition attributed to a CT state was clearly shown in the polymers. Interestingly, reversible thermo-responsiveness with generation of the broad absorption band in NIR region was observed in **P-BAz-3F** probably because of interaction between additional fluorine and nitrogen atoms. Furthermore, theoretical calculation well supported the interpretation of the effects gifted by fluorination. Through fluorinated BAz compounds, it was revealed that the influence of fluorination was systematically understandable and the fluorination was effective in controlling energy gaps of π-conjugated polymers. The study disclosed high potentiality of BAz compounds as a strong electron acceptor.

Supporting Information

Supporting Information is available from the Wiley Online Library or from the author.

Acknowledgements

This work was partially supported by the Mizuho Foundation for the Promotion of Sciences, Japan (for M.G.) and a Grant-in-Aid for Early-Career Scientists (for M.G.) (JSPS KAKENHI Grant numbers 20 K15334), for Scientific Research (B) (for K.T), (JP17H03067), for Scientific Research on Innovative Areas "New Polymeric Materials Based on Element-Blocks (No.2401)" (JP24102013) and for Challenging Research (Pioneering) (JP18H05356).

Conflict of Interest

The authors declare no conflict of interest.

Keywords: boron · conjugated polymer · NIR · solid-state emission · azobenzene

[1] a) A. X. Chen, A. T. Kleinschmidt, K. Choudhary, D. J. Lipomi, *Chem. Mater.* **2020**, *32*, 7582–7601; b) L. Giraud, S. Grelier, E. Grau, G. Hadziioannou, C. Brochon, H. Cramail, E. Cloutet, *J. Mater. Chem. C* **2020**, *8*, 9792–9810; c) R. H. Friend, R. W. Gymer, A. B. Holmes, J. H. Burroughes, R. N. Marks, C. Taliani, D. D. C. Bradley, D. A. D. Santos, J. L. Brédas, M. Lögdlund, W. R. Salaneck, *Nature* **1999**, *397*, 121–128; d) A. C. Grimsdale, K. Leok Chan, R. E. Martin, P. G. Jokisz, A. B. Holmes, *Chem. Rev.* **2009**, *109*, 897–1091; e) A. P. Kulkarni, C. J. Tonzola, A. Babel, S. A. Jenekhe, *Chem. Mater.* **2004**, *16*, 4556–4573; f) H. Zhou, L. Yang, W. You, *Macromolecules* **2012**, *45*, 607–632.

[2] a) H. Watanabe, K. Tanaka, Y. Chujo, *J. Org. Chem.* **2019**, *84*, 2768–2778; b) H. Watanabe, M. Hirose, K. Tanaka, K. Tanaka, Y. Chujo, *Polym. Chem.* **2016**, *7*, 3674–3680; c) H. Watanabe, J. Ochi, K. Tanaka, Y. Chujo, *Eur. J. Org. Chem.* **2020**, 777–783; d) Z. Genene, W. Mammo, E. Wang, M. R. Andersson, *Adv. Mater.* **2019**, *31*, 1807275; e) P. Cheng, Y. Yang, *Acc. Chem. Res.* **2020**, *53*, 1218–1228; f) B.-G. Kim, X. Ma, C. Chen, Y. Ie, E. W. Coir, H. Hashemi, Y. Aso, P. F. Green, J. Kieffer, J. Kim, *Adv. Funct. Mater.* **2013**, *23*, 439–445.

[3] a) B. C. Thompson, L. G. Madrigal, M. R. Pinto, T.-S. Kang, K. S. Schanze, J. R. Reynolds, *J. Polym. Sci. Part A* **2005**, *43*, 1417—1431; b) G. Tregnago, T. T. Steckler, O. Fenwick, M. R. Andersson, F. Cacialli, *J. Mater. Chem. C* **2015**, *3*, 2792–2797; c) T. T. Steckler, M. J. Lee, Z. Chen, O. Fenwick, M. R. Andersson, F. Cacialli, H. Sirringhaus, *J. Mater. Chem. C* **2014**, *2*, 5133–5141; d) T. T. Steckler, O. Fenwick, T. Lockwood, M. R. Andersson, F. Cacialli, *Macromol. Rapid Commun.* **2013**, *34*, 990–996.

[4] a) H.-H. Liu, S.-L. Chang, K.-H. Huang, F.-Y. Cao, K.-Y. Cheng, H.-S. Sun, Y.-Y. Lai, Y.-J. Cheng, *Macromolecules* **2020**, *53*, 7740–7748; b) D. Shi, Z. Liu, J. Ma, Z. Zhao, L. Tan, G. Lin, J. Tian, X. Zhang, G. Zhang, D. Zhang, *Adv. Funct. Mater.* **2020**, *30*, 1910235; c) C.-H. Chen, Y. Wang, T. Michinobu, S.-W. Chang, Y.-C. Chiu, C.-Y. Ke, G.-S. Liou, *ACS Appl. Mater. Interfaces* **2020**, *12*, 6144–6150; d) S. Jeon, C. Sun, S. H. Yu, S.-K. Kwon, D. S. Chung, Y. J. Jeong, Y.-H. Kim, *ACS Appl. Mater. Interfaces* **2020**, *12*, 2743–2752.

[5] a) H. L. T. Mai, N. T. T. Truong, T. Q. Nguyen, B. K. Doan, D. H. Tran, L.-T. T. Nguyen, W. Lee, J. W. Jung, M. H. Hoang, H. P. K. Huynh, C. D. Tran, H. T. Nguyen, *New J. Chem.* **2020**, *44*, 16900–16912; b) S. Ma, S. Wu, J. Zhang, Y. Song, H. Tang, K. Zhang, F. Huang, Y. Cao, *ACS Appl. Mater. Interfaces* **2020**, *12*, 51776–51784; c) S. Samson, J. Rech, L. Perdigón-Toro, Z. Peng, S. Shoaee, H. Ade, D. Neher, M. Stolterfoht, W. You, *ACS Appl. Polym. Mater.* **2020**, *2*, 5300–5308; d) R. Zhao, J. Liu, L. Wang, *Acc. Chem. Res.* **2020**, *53*, 1557–1567.

[6] a) G. Qian, Z. Y. Wang, *Chem. Asian J.* **2010**, *5*, 1006–1029; b) Y. Li, J.-D. Lin, X. Che, Y. Qu, F. Liu, L.-S. Liao, S. R. Forrest, *J. Am. Chem. Soc.* **2017**, *139*, 17114–17119.

[7] a) H. Xiang, J. Cheng, X. Ma, X. Zhou, J. J. Chruma, *Chem. Soc. Rev.* **2013**, *42*, 6128–6185; b) L. Yuan, W. Lin, K. Zheng, L. He, W. Huang, *Chem. Soc. Rev.* **2013**, *42*, 622–661; c) A. Zampetti, A. Minotto, F. Cacialli, *Adv. Funct. Mater.* **2019**, *29*, 1807623; d) N. Suzuki, M. Wakioka, F. Ozawa, S. Yamaguchi, *Asian J. Org. Chem.* **2020**, *9*, 1326–1332; e) S. Wang, J. Liu, G. Feng, L. G. Ng, B. Liu, *Adv. Funct. Mater.* **2019**, *29*, 1808365; f) C. Rohatgi, T. Harada, E. F. Need, M. Krasowska, D. A. Beattie, G. D. Dickenson, T. A. Smith, T. W. Kee, *ACS Appl. Nano Mater.* **2018**, *1*, 4801–4808; g) L. Chen, D. Chen, Y. Jiang, J. Zhang, J. Yu, C. C. DuFort, S. R. Hingorani, X. Zhang, C. Wu, D. T. Chiu, *Angew. Chem. Int. Ed.* **2019**, *58*, 7008–7012; *Angew. Chem.* **2019**, *131*, 7082–7086; h) G. Deng, X. Peng, Z. Sun, W. Zheng, J. Yu, L. Du, H. Chen, P. Gong, P. Zhang, L. Cai, B. Z. Tang, *ACS Nano* **2020**, *14*, 11452–11462; i) P. R. Neumann, D. L. Crossley, M. Turner, M. Ingleson, M. Green, J. Rao, L. A. Dailey, *ACS Appl. Mater. Interfaces* **2019**, *11*, 46525–46535; j) X. Ma, X. Jiang, S. Zhang, X. Huang, Y. Cheng, C. Zhu, *Polym. Chem.* **2013**, *4*, 4396–4404; k) R. Yoshii, A. Nagai, Y. Chujo, *J. Polym. Sci. Part A* **2010**, *48*, 5348–5356; l) R. Yoshii, A. Nagai, K. Tanaka, Y. Chujo, *J. Polym. Sci. Part A* **2013**, *51*, 1726–1733.

[8] a) D. M. de Leeuw, M. M. J. Simenon, A. R. Brown, R. E. F. Einerhand, *Synth. Met.* **1997**, *87*, 53–59; b) V. Viswanathan, A. Rao, U. Pandey, A. V. Kesavan, P. Ramamurthy, *Beilstein J. Org. Chem.* **2017**, *13*, 863–873.

[9] a) F. Babudri, G. M. Farinola, F. Naso, R. Ragni, *Chem. Commun.* **2007**, 1003–1022; b) H. Zhou, L. Yang, A. C. Stuart, S. C. Price, S. Liu, W. You, *Angew. Chem. Int. Ed.* **2011**, *50*, 2995–2998; *Angew. Chem.* **2011**, *123*, 3051–3054; c) H. J. Son, W. Wang, T. Xu, Y. Liang, Y. Wu, G. Li, L. Yu, *J. Am. Chem. Soc.* **2011**, *133*, 1885–1894; d) D. Deng, Y. Zhang, J. Zhang, Z. Wang, L. Zhu, J. Fang, B. Xia, Z. Wang, K. Lu, W. Ma, Z. Wei, *Nat. Commun.* **2016**, *7*, 13740; e) M. Zhang, X. Guo, S. Zhang, J. Hou, *Adv. Mater.* **2014**, *26*, 1118–1123; f) N. Wang, Z. Chen, W. Wei, Z. Jiang, *J. Am. Chem. Soc.* **2013**, *135*, 17060–17068; g) T. Lei, J.-H. Dou, Z.-J. Ma, C.-H. Yao, C.-J. Liu, J.-Y. Wang, J. Pei, *J. Am. Chem. Soc.* **2012**, *134*, 20025–20028; h) T. Lei, X. Xia, J.-Y. Wang, C.-J. Liu, J. Pei, *J. Am. Chem. Soc.* **2014**, *136*, 2135–2141; i) D. Liu, W. Zhao, S. Zhang, L. Ye, Z. Zheng, Y. Cui, Y. Chen, J. Hou, *Macromolecules* **2015**, *48*, 5172–5178; j) P. Lei, B.

Zhang, Y. Chen, Y. Geng, Q. Zeng, A. Tang, E. Zhou, *ACS Appl. Mater. Interfaces* **2020**, *12*, 38451–38459.

[10] a) Y. Chujo, K. Tanaka, *Bull. Chem. Soc. Jpn.* **2015**, *88*, 633–643; b) M. Gon, K. Tanaka, Y. Chujo, *Polym. J.* **2018**, *50*, 109–126; c) K. Tanaka, Y. Chujo, *Polym. J.* **2020**, *52*, 555–566.

[11] a) M. Gon, K. Tanaka, Y. Chujo, *Chem. Rec.* **2021**, *21*, DOI: 10.1002/tcr.202000156; b) M. Gon, K. Tanaka, Y. Chujo, *Angew. Chem. Int. Ed.* **2018**, *57*, 6546–6551; *Angew. Chem.* **2018**, *130*, 6656–6661; c) S. Ohtani, M. Gon, K. Tanaka, Y. Chujo, *Macromolecules* **2019**, *52*, 3387–3393; d) M. Gon, J. Wakabayashi, K. Tanaka, Y. Chujo, *Chem. Asian J.* **2019**, *14*, 1837–1843; e) M. Gon, J. Wakabayashi, M. Nakamura, K. Tanaka, Y. Chujo, *Macromol. Rapid Commun.* **2020**, 2000566, DOI:10.1002/marc.202000566.

[12] S. A. Jenekhe, J. A. Osaheni, *Science* **1994**, 265, 765–768.

[13] a) S. Ohtani, M. Gon, K. Tanaka, Y. Chujo, *Chem. Eur. J.* **2017**, *23*, 11827–11833; b) S. Ohtani, M. Nakamura, M. Gon, K. Tanaka, Y. Chujo, *Chem. Commun.* **2020**, *56*, 6575–6578; c) S. Ohtani, M. Gon, K. Tanaka, Y. Chujo, *Crystals* **2020**, *10*, 615; d) S. Ohtani, Y. Takeda, M. Gon, K. Tanaka, Y. Chujo, *Chem. Commun.* **2020**, *56*, 15305–15308; e) J. Wakabayashi, M. Gon, K. Tanaka, Y. Chujo, *Macromolecules* **2020**, *53*, 4524–4532.

[14] a) J. Mei, N. L. C. Leung, R. T. K. Kwok, J. W. Y. Lam, B. Z. Tang, *Chem. Rev.* **2015**, *115*, 11718–11940; b) J. Luo, Z. Xie, J. W. Y. Lam, L. Cheng, H. Chen, C. Qiu, H. S. Kwok, X. Zhan, Y. Liu, D. Zhu, B. Z. Tang, *Chem. Commun.* **2001**, 1740–1741.

[15] Y. Dong, J. W. Y. Lam, A. Qin, Z. Li, J. Sun, H. H.-Y. Sung, I. D. Williams, B. Z. Tang, *Chem. Commun.* **2007**, 40–42.

[16] a) C.-L. Liu, F.-C. Tsai, C.-C. Chang, K.-H. Hsieh, J.-L. Lin, W.-C. Chen, *Polymer* **2005**, *46*, 4950–4957; b) Y. Wang, J. Ma, Y. Jiang, *J. Phys. Chem. A* **2005**, *109*, 7197–7206.

[17] a) M. Kosugi, K. Sasazawa, Y. Shimizu, T. Migita, *Chem. Lett.* **1977**, *6*, 301–302; b) D. Milstein, J. K. Stille, *J. Am. Chem. Soc.* **1978**, *100*, 3636–3638.

[18] M. Gon, K. Tanaka, Y. Chujo, *Bull. Chem. Soc. Jpn.* **2019**, *92*, 7–18.

[19] X. Long, Z. Ding, C. Dou, J. Zhang, J. Liu, L. Wang, *Adv. Mater.* **2016**, *28*, 6504–6508.

[20] K. Suenaga, K. Uemura, K. Tanaka, Y. Chujo, *Polym. Chem.* **2020**, *11*, 1127–1133.

[21] a) J. Pommerehne, H. Vestweber, W. Guss, R. F. Mahrt, H. Bässler, M. Porsch, J. Daub, *Adv. Mater.* **1995**, *7*, 551–554; b) C. M. Cardona, W. Li, A. E. Kaifer, D. Stockdale, G. C. Bazan, *Adv. Mater.* **2011**, *23*, 2367–2371.

Manuscript received: January 14, 2021
Revised manuscript received: January 31, 2021
Accepted manuscript online: February 1, 2021
Version of record online: February 12, 2021